Accepted Manuscript

Design of bisquinolinyl malonamides as Zn^{2+} ion-selective fluoroionophores based on the substituent effect

Takayo Moriuchi-Kawakami , Keita Kawata , Sho Nakamura , Yoshiaki Koyama , Yasuhiko Shibutani

PII: S0040-4020(14)01574-9

DOI: 10.1016/j.tet.2014.11.016

Reference: TET 26165

To appear in: *Tetrahedron*

Received Date: 18 August 2014

Revised Date: 4 November 2014

Accepted Date: 6 November 2014

Please cite this article as: Moriuchi-Kawakami T, Kawata K, Nakamura S, Koyama Y, Shibutani Y, Design of bisquinolinyl malonamides as Zn^{2+} ion-selective fluoroionophores based on the substituent effect, *Tetrahedron* (2014), doi: 10.1016/j.tet.2014.11.016.

Graphical Abstract

Design of bisquinolinyl malonamides as Zn^{2+} ion-selective fluoroionophores based on the substituent effect

Leave this area blank for abstract info.

Takayo Moriuchi-Kawakami,* Keita Kawata, Sho Nakamura, Yoshiaki Koyama, Yasuhiko Shibutani
Department of Applied Chemistry, Faculty of Engineering, Osaka Institute of Technology

The substituents introduced into the C2-position of malonamides are spatially distant from the recognition moiety quinoline but influenced their ion selectivities greatly.

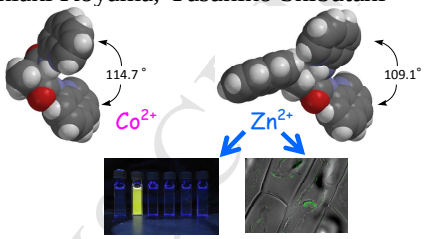

Tetrahedron
journal homepage: www.elsevier.com

Design of bisquinolinyl malonamides as Zn^{2+} ion-selective fluoroionophores based on the substituent effect

Takayo Moriuchi-Kawakami*, Keita Kawata, Sho Nakamura, Yoshiaki Koyama and Yasuhiko Shibutani

Department of Applied Chemistry, Faculty of Engineering, Osaka Institute of Technology, 5-16-1Omiya, Asahi, Osaka 535-8585, Japan

ARTICLE INFO

Article history:
Received
Received in revised form
Accepted
Available online

Keywords:
Zn^{2+} ion-selective
fluoroionophore
malonamide
substituent effect
visible analysis

ABSTRACT

A series of malonamides possessing two quinoline moieties were synthesized and characterized as fluoroionophores for the Zn^{2+} ion. We focused on the relationship between the substituents introduced to the C2-position of the malonamides and their Zn^{2+} ion-selectivity, exploiting the structural effect of the substituents in the design of the fluoroionophores with high selectivity. The substituents introduced to the malonamides were the methyl, benzyl, and naphthalenylmethyl groups. In dimethyl sulfoxide solvent, all substituted bisquinolinyl malonamides showed excellent fluorescence sensing for the Zn^{2+} ion, while unsubstituted bisquinolinyl malonamide **1** displayed ratiometric sensing for the Co^{2+} ion. *N*, *N*'-bis(8-quinolyl)-2-methyl-2-naphthalenylmethyl malonamide **4** exhibited the highest Zn^{2+} ion-selectivity against the Cd^{2+} ion. Although the substituents introduced into the C2-position are spatially distant from the quinoline recognition moiety, this study indicated that they greatly influenced the ion selectivities of the bisquinolinyl malonamides. Furthermore, it was demonstrated that visible fluorescence analyses could be performed on malonamide **4**.

1. Introduction

In the last few decades, studies on molecular probes which act as optical switches for the Zn^{2+} ion have greatly increased.[1] Such rapid development is derived from an understanding of the roles played by the Zn^{2+} ion in biological processes.[2] The Zn^{2+} ion is the second most abundant transition metal in the human body behind iron, and its biological roles are diverse and important. Although most of the Zn^{2+} ions in vivo are contained within peptides or proteins, the physiological roles of the free Zn^{2+} ion have attracted much attention. Hence, there is a need to detect the Zn^{2+} ion easily and selectively. However, it is still a challenge to develop simple and useful methods for the selective detection of the Zn^{2+} ion against such interference ions as the Cd^{2+} ion since Cd^{2+} and Cu^{2+} ions have similar properties in their interaction with ionophores.[3]

Most of the fluoroionophores for cation sensing are composed of a cation recognition site with a fluorescent moiety.[4] Along with di-2-picolylamine (DPA) and bipyridine, quinoline derivatives (particularly 8-hydroxyquinoline or 8-amino quinoline) is one of the most useful fluorescent units for the detection of the Zn^{2+} ion.[1] In fact, the 8-aminoquinoline derivative, *N*-(6-methoxy-8-quinolyl)-*p*-toluenesulfonamide (TSQ), is commercially available and most widely used for the imaging of Zn^{2+} ions.[5] In this study, we have focused on the design and synthesis of Zn^{2+} ion-selective fluoroionophores based on the substituent effect. It was evident through our work that the substituents introduced into the C2-position of malonamides greatly influenced their ion selectivities, although the introduced substituents are spatially distant from the recognition moiety quinoline and do not participate directly in ion-sensing.

2. Results and discussion

2.1. Syntheses of malonamides and fluorescence responses

Unsubstituted malonamide **1** was prepared by the synthetic routes depicted in Fig. 1 and its fluorescence response was examined. The reaction of the unsubstituted malonyl dichloride with 8-aminoquinoline in toluene afforded the desired derivative **1**.

Fig. 2a shows the fluorescence spectra (excitation wavelength: λ_{ex} = 345 nm) of the unsubstituted malonamide **1** (5.0×10^{-6} M) measured using dimethyl sulfoxide (DMSO) solution in the absence or presence of 1 equiv. of each respective cation. Malonamide **1** itself shows fluorescence at 408 nm. The addition of the Zn^{2+} and Cd^{2+} ions to the solution led to a decrease in the fluorescence and the appearance of a red-shifted fluorescence at 529 nm. The fluorescence intensity at 529 nm in the presence of the Cd^{2+} ions was stronger by 1.4-fold to that in

* Corresponding author. Tel.: +81-6-6954-4281; fax: +81-6-6957-2135; e-mail: kawakami@chem.oit.ac.jp (T. Moriuchi-Kawakami)

the presence of the Zn^{2+} ions (F_{Cd}/F_{Zn} = 1.4). The addition of the Co^{2+} ion strongly quenches the fluorescence at 408 nm and afforded a red-shifted fluorescence at 486 nm. Furthermore, the fluorescence intensity at 486 nm in the presence of Co^{2+} ions was stronger by 1.7-fold to that at 529 nm over Zn^{2+} (F_{Co}/F_{Zn} = 1.7). In contrast, the addition of other cations (Li^+, Na^+, K^+, NH_4^+, Mg^{2+}, Ca^{2+}, Al^{3+}, Mn^{2+}, Ni^{2+}, Cu^{2+}, Ag^+) did not lead to the appearance of red-shifted fluorescence, although some cations somewhat decreased the fluorescence at 408 nm.

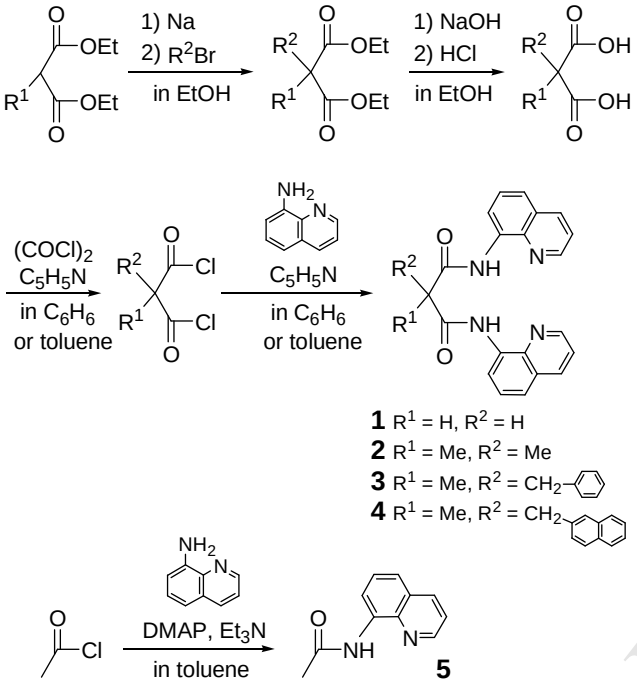

Fig. 1. Syntheses of malonamide derivatives **1** – **4** and amide **5**.

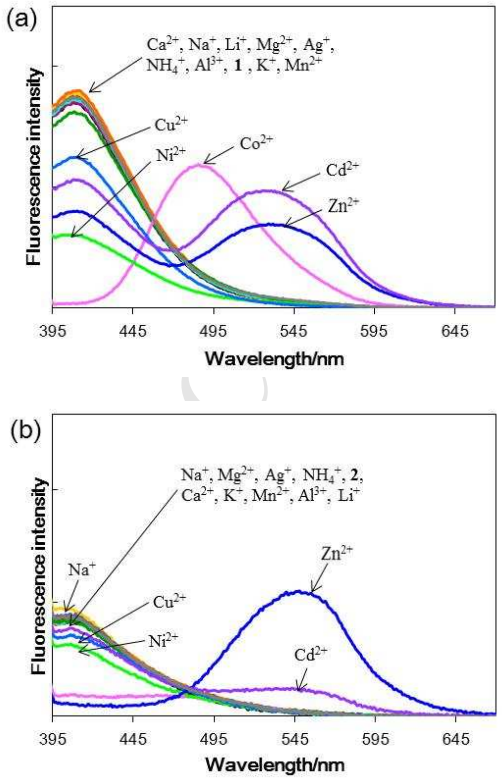

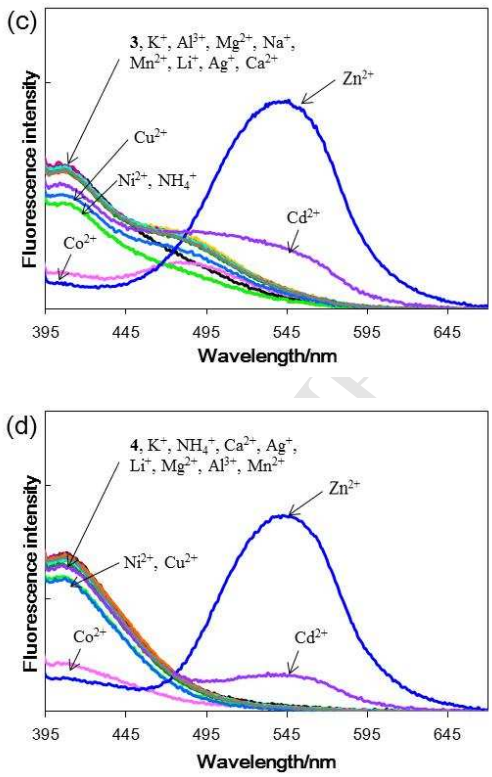

Fig. 2. Fluorescence spectra of malonamides **1**– **4** (5 μM) in the presence of 1 equiv. of Li^+, Na^+, K^+, NH_4^+, Mg^{2+}, Ca^{2+}, Al^{3+}, Mn^{2+}, Co^{2+}, Ni^{2+}, Cu^{2+}, Zn^{2+}, Cd^{2+}, and Ag^+ in DMSO (excitation wavelength: λ_{ex} = 345 nm): a) **1**, b) **2**, c) **3**, d) **4**.

Here, we exploited the structural effect of the substituents at the C2-position of malonamides in the design of fluoroionophores for the Zn^{2+} ion. One important factor in the ion selectivity of bisquinolinyl malonamides is the orientation of two quinoline rings as the recognition moieties. The different orientations of two quinoline rings will lead the difference of ion selectivities of bisquinolinyl malonamides. We expected the orientations of two quinoline rings will vary with the steric hindrance of the sp^3 carbon in the C2-position of malonamides. Therefore, in consideration of the steric hindrance, the methyl, benzyl, and naphthalenylmethyl groups were selected as the substituents introduced to the C2-position of the malonamides. Disubstituted malonamides **2** – **4** were prepared by the synthetic routes depicted in Fig. 1. Malonic acid dichlorides were synthesized by the reaction of corresponding malonic acids with ($COCl_2$) in benzene or toluene.[6,7] Subsequently, the reaction of malonic acid dichlorides with 8-aminoquinoline in benzene or toluene resulted in the desired malonamides **2** – **4**. The fluorescence responses of the disubstituted malonamides **2** – **4** were investigated in the absence or presence of 1 equiv. of each respective cation.

As shown in Fig. 2b, the fluorescence spectra of malonamide **2** possessing two methyl substituents indicated that the addition of the Zn^{2+} ion significantly decreased the fluorescence of malonamide **2** itself at 405 nm along with the distinct appearance of red-shifted fluorescence at 548 nm. The addition of other cations, except the Cd^{2+} ion, merely showed slight spectral changes at 405 nm. The addition of the Cd^{2+} ion led to the slight appearance of a red-shifted fluorescence at 548 nm with no decrease in the fluorescence at 405 nm. The fluorescence intensity at 548 nm in the presence of the Zn^{2+} ions was stronger

by 4.8-fold to that over Cd^{2+} (F_{Zn}/F_{Cd} = 4.8). The introduction of the substituents at the C2-position was effective for the recognition of the Zn^{2+} ion with high selectivity. In the case of malonamide **3** possessing the methyl and benzyl groups as substituents at the C2-position, the addition of the Zn^{2+} ion, in a likewise manner, markedly decreased the fluorescence of malonamide **3** itself at 407 nm and the clear appearance of a red-shifted fluorescence at 544 nm was observed (Fig. 2c). However, the fluorescence intensity at 544 nm in the presence of the Zn^{2+} ions was superior by 3.5-fold over the Cd^{2+} ions (F_{Zn}/F_{Cd} = 3.5). On the other hand, in the case of malonamide **4** possessing the methyl and naphthalenylmethyl groups, the addition of Zn^{2+} largely decreased the fluorescence of malonamide **4** itself at 408 nm while the appearance of a sharp red-shifted fluorescence was observed at 542 nm (Fig. 2d). The fluorescence intensity at 542 nm in the presence of the Zn^{2+} ions was stronger by 5.5-fold to that over Cd^{2+} (F_{Zn}/F_{Cd} = 5.5). The F_{Zn}/F_{Cd} values of the fluorescence intensities in the presence of the Zn^{2+} ions compared with those over Cd^{2+} increased in the order of malonamide **1** << **3** < **2** < **4**, as summarized in Table 1. The Zn^{2+} ion-selectivity against the Cd^{2+} ion of malonamide **4** was the highest among malonamides **1** – **4**. Hirata et al. demonstrated that malonamide analogs with the benzyl substituent can selectively extract the Cu^{2+} ion into chloroform from an aqueous mixture of Cu^{2+}, Ni^{2+}, Co^{2+} and Zn^{2+} ions.[8] However, in this study, no selective fluorescence performance of malonamides **1** – **4** to the Cu^{2+} ion was observed. Artaud et al. reported that the substituents introduced to the C2-position of malonamide analogs determined the *cis* or *trans* orientations of the complexes with the metal ions.[9,10] Therefore, the difference in the substituents may influence the fluorescence performances.

Table 1
Ion-selective fluorescence performance of malonamides **1** – **4** to Zn^{2+} and Cd^{2+} in DMSO

malonamide	F_{Zn} / F_{Cd}	R_{Zn}	R_{Cd}
1	0.7 (at 529 nm)	0.87 (F_{529}/ F_{408})	0.91 (F_{529}/ F_{408})
2	4.7 (at 548 nm)	10.43 (F_{548}/ F_{405})	0.30 (F_{548}/ F_{405})
3	3.5 (at 544 nm)	7.98 (F_{544}/ F_{407})	0.49 (F_{544}/ F_{407})
4	5.5 (at 542 nm)	5.88 (F_{542}/ F_{408})	0.25 (F_{542}/ F_{408})

For comparison, derivative **5** possessing only one quinoline moiety was also prepared by a similar method (Fig. 1) and the fluorescence spectra of amide **5** was measured using a DMSO solution in the absence or presence of 1 equiv. of each respective cation. The fluorescence spectra of amide **5** showed no change with the addition of the investigated cations (Fig. S1). These results suggest that two quinolyl amide moieties are necessary for ion recognition[11] and that a sandwich-type coordination has an advantage in ion recognition.[12]

Fluorescence titration experiments were performed using DMSO solutions to investigate the quantitative performance for the Zn^{2+} ion. In the fluorescence titration study, the fluorescence intensities were measured in different concentrations of the Zn^{2+} ion against standard 5 μM malonamides **1** – **4**. The intrinsic fluorescence emissions of bisquinolinyl malonamides at ca. 400 nm decreased and these were accompanied by the increases in fluorescence excitations at ca. 540 nm (Fig. 3). The fluorescence intensities at ca. 540 nm were linearly increased in the initial part of the titration as shown in the insets of Fig. 3. The results revealed that there is an affinity between malonamides **1** – **4** and the Zn^{2+} ion.

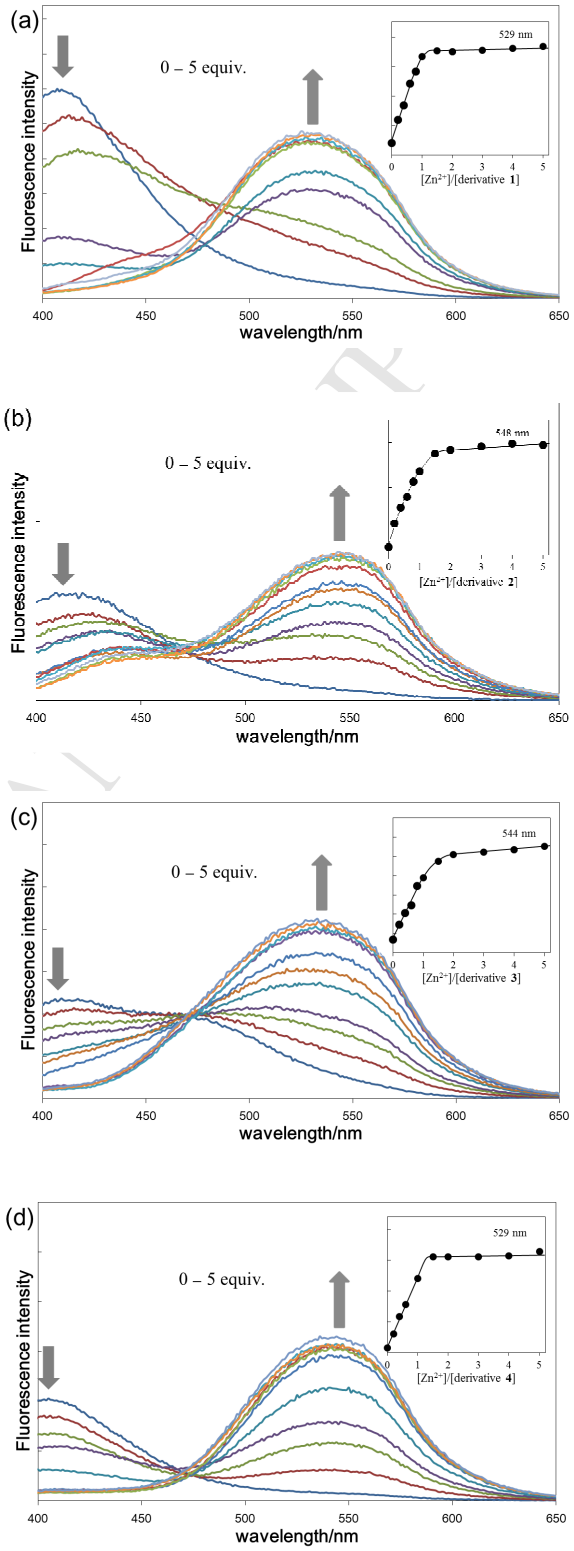

Fig. 3. Fluorescence spectra of malonamides **1**– **4** (5 μM) obtained during titration by Zn^{2+} ion (0, 0.2, 0.4, 0.6, 0.8, 1.0, 1.5, 2.0, 3.0, 4.0, 5.0 equiv.) in DMSO (excitation wavelength: λ_{ex} = 345 nm): a) **1**, b) **2**, c) **3**, d) **4**. Inset: titration curves of the fluorescence intensities as functions of [Zn^{2+}]/[malonamide derivatives].

On the fluorescence emission of fluoroionophores with the Zn^{2+} ion, it is well-established that excited states resulting from

complexes of zinc (II) are typically ligand-centered (LC) in nature, owing to the inability of the d^{10} metal center to participate in low energy charge transfer or metal-centered transitions.[13-15] Malonamides **1** – **4** and derivative **5** contain amino-substituted quinolone moiety which are candidates for fluorophores with photo-induced electron transfer (PeT) mechanism.[16-18] However, derivatives **1** – **4** and **5** fluoresced, respectively, without PeT quenching pathway. Moreover, the derivative **5** exhibited no new emission band by adding the Zn^{2+} ion or other metal ions. Therefore, the new emission bands (ca. 540 nm) of malonamides **1** – **4** by adding the Zn^{2+} ion would arise from two effects: first, the binding of malonamides **1** – **4** to the Zn^{2+} ion, which occurs with two aminoquinoline moieties through two aromatic nitrogen atoms, will reduces the energy difference between *n* and π^* orbital (internal charge transfer (ICT)).[19-23] Second, the aminoquinoline moiety, which is proximate with one another as a consequence of the binding, may form the π – π stacking interactions, resulting the fluorescence enhancement and the red-shifted emission bands.[24-28]

2.2. Ratiometric responses

We further also examined the ratiometric fluorescence responses of bisquinolinyl malonamide derivatives. Most fluoroionophores for the Zn^{2+} ion can detect with an increase in the emission intensity.[1] However, it is desirable to eliminate the effects of these factors by using ratiometry since the emission intensity is also dependent on various other factors.[29] A ratiometric fluoroionophore not only exhibits a spectral shift, but also provides ratiometric measurement in the emission intensities of two emission wavelengths.

The obtained spectral data indicated that malonamide **1** selectively showed ratiometric fluorescence response to the Co^{2+} ion in DMSO (Fig. S2a). In fact, the fluorescence intensity ratios (F_{486}/F_{408}) at 486 nm to that at 408 nm was R_{Co} = 30.9 on the Co^{2+} ion. Even the fluorescence intensity ratios (F_{529}/F_{408}) at 529 nm to that at 408 nm on the Co^{2+} ion (R_{Co} = 15.7) was superior to that on the Cd^{2+} ion (R_{Cd} = 0.9). In contrast, the fluorescence intensity ratios (F_{548}/F_{405}) of malonamide **2** at 548 nm to that at 405 nm were R_{Zn} = 10.4 on the Zn^{2+} ion and R_{Cd} = 0.3 on the Cd^{2+} ion (Fig. S2b and Table 1). As shown in Table 1, this is the best ratiometric fluorescence response to the Zn^{2+} ion among malonamides **1** – **4**. On the other hand, the fluorescence intensity ratios (F_{544}/F_{407}) of malonamide **3** at 544 nm to that at 407 nm were R_{Zn} = 8.0 on the Zn^{2+} ion and R_{Cd} = 0.5 on the Cd^{2+} ion (Fig. S2c and Table 1). The fluorescence intensity ratios (F_{542}/F_{408}) of malonamide **4** were R_{Zn} = 5.9 on the Zn^{2+} ion and R_{Cd} = 0.3 on the Cd^{2+} ion (Fig. S2d and Table 1). The F_{Zn}/F_{Cd} values of the fluorescence intensities in the presence of Zn^{2+} ions as compared with Cd^{2+} increased in the order of malonamide **1** << **3** < **2** < **4**, while the R_{Zn}/R_{Cd} values for the ratiometric fluorescence performance increased in the order of malonamide **1** << **4** < **3** < **2**. The ratiometric fluorescence performance of malonamide **4** in the presence of Zn^{2+} ion was inferior to that of malonamide **2** since the addition of Zn^{2+} did not entirely quench the fluorescence of malonamide **4** itself at 407 nm.

2.3. Solvent effects

Chen et al. investigated the fluorescence response of malonamide **1** in dimethylformamide (DMF) solution and reported that malonamide **1** displayed superior Zn^{2+} ion selectivity against the Pb^{2+}, Cu^{2+}, Co^{2+}, Ni^{2+} ions.[30] We also examined the fluorescence response of malonamide **1** – **4** using a DMF solvent (excitation wavelength: λ_{ex} = 320 nm). In the case of malonamide **1**, the F_{Zn}/F_{Cd} value of the fluorescence intensities for the Zn^{2+} ion against the Cd^{2+} ion was 1.7 (F_{Zn}/F_{Cd} = 1.7) and malonamide **1** actually displayed favorable Zn^{2+} ion selectivity. In all of the malonamides **1** – **4**, the F_{Zn}/F_{Cd} values determined using a DMF solvent were superior to those using the DMSO solvent (Fig. S3). Unlike DMSO solvent, the F_{Zn}/F_{Cd} values of the fluorescence intensities for the Zn^{2+} ion against the Cd^{2+} ion increased in the order of malonamide **1** < **2** < **3** < **4**. However, the favorable results were not always obtained, in particular when the concentration was large. Our further investigations led to the result that the complexes between malonamides and the Zn^{2+} ion gradually form precipitates in the DMF solvent. Although the fluorescence response of malonamide **4** using a $CH_3CN/CHCl_3$ solvent (9:1, v/v) (excitation wavelength: λ_{ex} = 319 nm) was also examined, malonamide **4** displayed inferior Zn^{2+} ion selectivity against the Cd^{2+} and Cu^{2+} ions (F_{Zn}/F_{Cd} = 0.64 and F_{Zn}/F_{Cu} = 0.76) (Fig. S4). We, therefore, employed DMSO as the solvent for further study.

2.4. Coordination and absorption properties

In order to investigate the coordination of malonamides **1** – **4** with the Zn^{2+}, Cd^{2+} and Co^{2+} ions, spectrophotometric titrations were performed in DMSO solution. Upon the gradual addition of the metal ions (0.0 – 5.0 equiv.), all UV-vis spectra of malonamides **1** – **4** showed isosbestic points and an increase in the band at ca. 390 nm with no gradual shift (Fig. 4 – 7). For example, the UV-vis spectra of malonamide **1** with the addition of the Zn^{2+} ion also exhibited isosbestic points at 288 and 345 nm and an increase in the band at 385 nm (Fig. 4a), although the fluorescence response to the Zn^{2+} ions of malonamide **1** was inferior to that towards the Cd^{2+} and Co^{2+} ions.

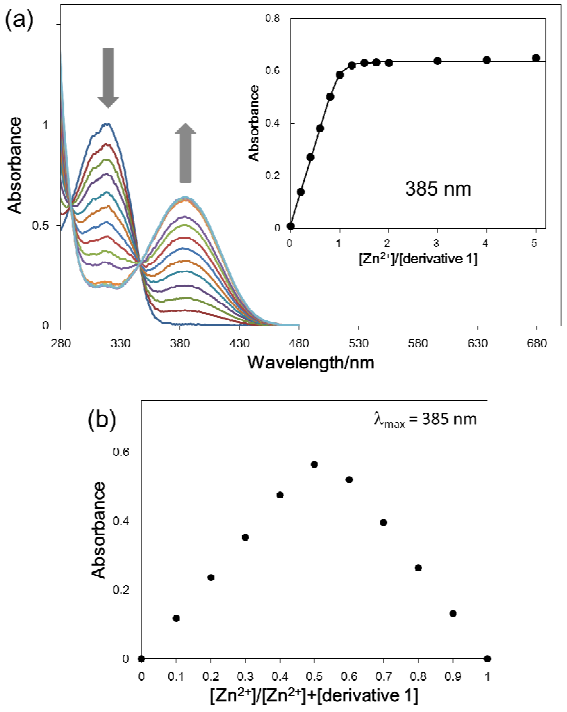

Fig. 4. a) UV-vis absorption spectra and absorbance changes at 385 nm (inset) of malonamide **1** (0.8 mM) obtained during titration by the Zn^{2+} ion (0 – 5.0 equiv.) in DMSO. b) Job's plots of malonamide **1** with the Zn^{2+} ion according to the method for continuous variations in absorption in DMSO (total concentration of malonamide **1** and the Zn^{2+} ion is 0.16 mM).

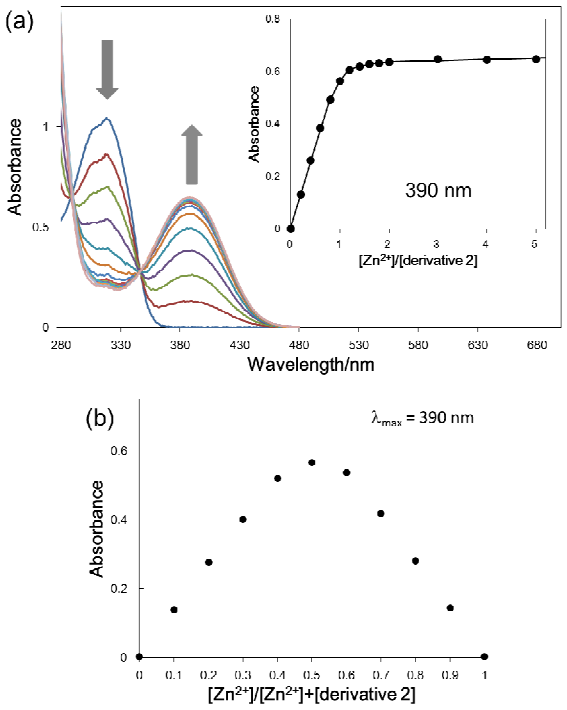

Fig. 5. a) UV-vis absorption spectra and absorbance changes at 390 nm (inset) of malonamide **2** (0.8 mM) obtained during titration by the Zn^{2+} ion (0 – 5.0 equiv.) in DMSO. b) Job's plots of malonamide **2** with the Zn^{2+} ion according to the method for continuous variations in absorption in DMSO (total concentration of malonamide **2** and the Zn^{2+} ion is 0.16 mM).

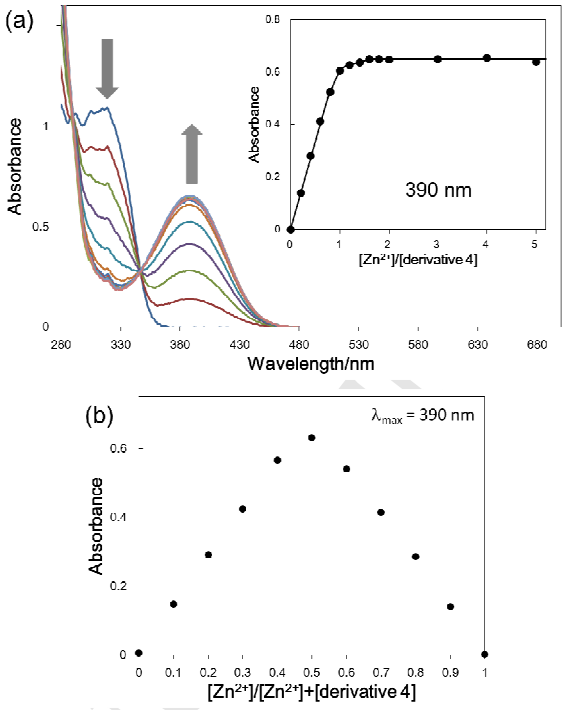

Fig. 7. a) UV-vis absorption spectra and absorbance changes at 390 nm (inset) of malonamide **4** (0.8 mM) obtained during titration by the Zn^{2+} ion (0, 0.2, 0.4, 0.6, 0.8, 1.0, 1.2, 1.4, 1.6, 1.8, 2.0, 3.0, 4.0, 5.0 equiv.) in DMSO. b) Job's plots of malonamide **4** with the Zn^{2+} ion according to the method for continuous variations in absorption in DMSO (total concentration of malonamide **4** and the Zn^{2+} ion is 0.16 mM).

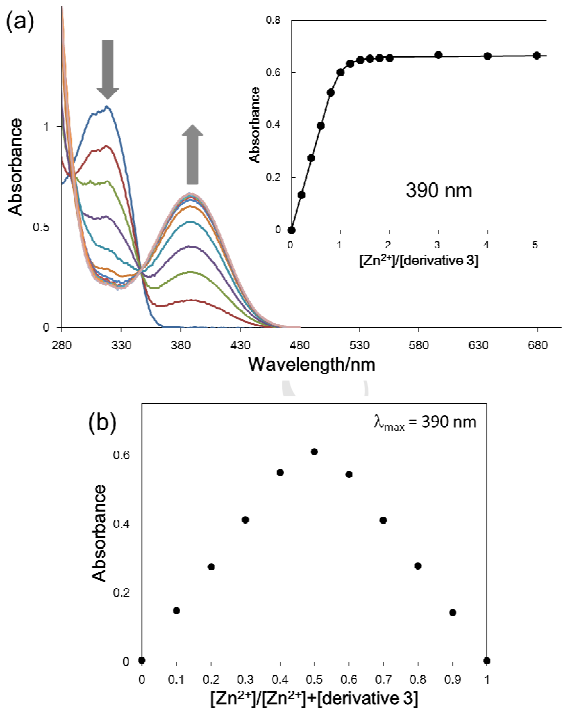

Fig. 6. a) UV-vis absorption spectra and absorbance changes at 390 nm (inset) of malonamide **3** (0.8 mM) obtained during titration by the Zn^{2+} ion (0 – 5.0 equiv.) in DMSO. b) Job's plots of malonamide **3** with the Zn^{2+} ion according to the method for continuous variations in absorption in DMSO (total concentration of malonamide **3** and the Zn^{2+} ion is 0.16 mM).

On the other hand, upon the addition of the Zn^{2+} ion, the UV-vis spectra of malonamide **4** exhibited isosbestic points at 290 and 344 nm and an increase in the band at 390 nm (Fig. 7a). These results indicate that a new species is produced by complexation with the Zn^{2+}, Cd^{2+} and Co^{2+} ions during titration.

In order to understand the complexation of malonamides **1** – **4** with the Zn^{2+}, Cd^{2+} and Co^{2+} ions, Job's plots for the absorbance were determined by keeping the sum of the initial concentrations of the malonamides and metal ions constant at 1.6×10^{-6} M and changing the molar ratio of the metal ions (X_M = $[M^{2+}]/([M^{2+}]+[\text{derivative}])$) from 0 to 1.[31] Fig. 4b – 7b depict Job's plots of malonamides **1** – **4** with the Zn^{2+} ion. All of the plots for the absorbance at ca. 390 nm versus the molar ratio of the metal ions X_M (M^{2+} = Zn^{2+}, Cd^{2+} and Co^{2+}) showed that the absorbance value is highest at the molar fraction of ca. 0.5, indicating that a 1:1 stoichiometry is most probable for the binding mode of malonamides **1** – **4** to the Zn^{2+}, Cd^{2+} and Co^{2+} ions.

Based on Job's-plot determination of 1:1 binding stoichiometry, the binding constants (*K*) of malonamides **1** – **4** to the Zn^{2+}, Cd^{2+} and Co^{2+} ions were respectively calculated from the titration data in UV-vis absorption (Fig. 4a – 7a inset, Fig. S5, Fig. S6) by means of a nonlinear least-squares method (Table 2).[32] All binding constants of malonamides **1** – **4** to the Zn^{2+} ion were superior to that of the Cd^{2+} ion. Surprisingly, the highest binding constants for malonamides **1** – **3**, but not malonamide **4**, were observed for the Co^{2+} ion as compared with the Zn^{2+} and Cd^{2+} ions. In particular, malonamide **1**, which exhibited excellent ratiometric fluorescence response to the Co^{2+} ion, had the highest binding constant to the Co^{2+} ion. The values of the binding

constants to the Zn^{2+} ion increased in the order of malonamide **2** < **1** < **3** < **4**. In fluorescence spectrometry, the highest Zn^{2+} ion-selectivity against the Cd^{2+} and Co^{2+} ions of malonamide **4** among the other malonamide derivatives was probably caused by the highly binding constant of malonamide **4** to the Zn^{2+} ion as compared with the Cd^{2+} and Co^{2+} ions.

Table 2
Stability constants *K* for complex formation between malonamides **1** – **4** and the Zn^{2+}, Cd^{2+} and Co^{2+} ions in DMSO

malonamide	metal ion	*K* (M^{-1})
1	Zn^{2+}	1.22×10^5
	Cd^{2+}	5.89×10^3
	Co^{2+}	3.07×10^5
2	Zn^{2+}	1.14×10^5
	Cd^{2+}	2.50×10^3
	Co^{2+}	2.15×10^5
3	Zn^{2+}	1.51×10^5
	Cd^{2+}	3.28×10^3
	Co^{2+}	2.39×10^5
4	Zn^{2+}	1.99×10^5
	Cd^{2+}	4.84×10^3
	Co^{2+}	1.64×10^5

2.5. Computational studies

In order to understand the structural effect of the substituents introduced into malonamides **2** – **4** on ion recognition, conformational analysis of the free malonamides **1** – **4** was performed by the semi-empirical (PM3) method.[6,33-35] For the semi-empirical molecular orbital calculations of the free bisquinolinyl malonamides, the structure of malonamides having all four 8-quinolinyl N atoms directed inward towards the cavity was employed as the starting geometries. Calculations for free malonamides **1** – **4** indicated that the dihedral angles between two quinoline rings varied according to the introduced substituents at the C2-position of the malonamides (Fig. 8).

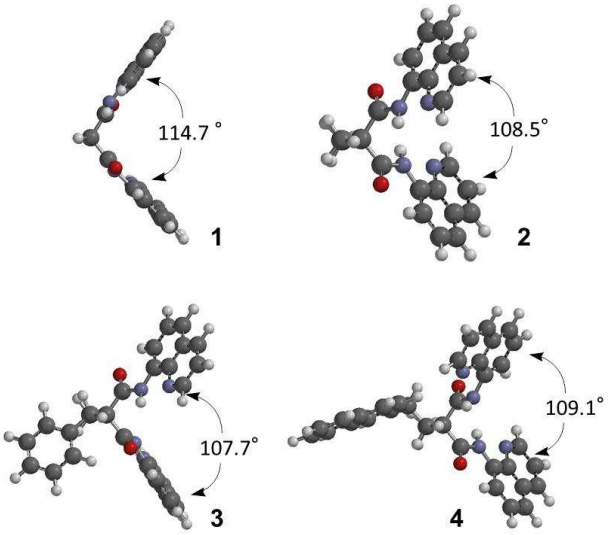

Fig. 8. Optimized conformations of malonamides **1** – **4**.

The values of the dihedral angles between two quinoline rings increased in the order of malonamide **3** < **2** < **4** < **1**. These results demonstrated that the substituents introduced into the C2-position affect the dihedral angles between the two quinoline rings and greatly influenced the ion selectivities of bisquinolinyl malonamides although the introduced substituents are spatially distant from the quinoline recognition moiety spatially and do not directly participate in ion-sensing. This C2-modification method of the bisquinolinyl malonamides seems to be applicable to the molecular design of various malonamide derivatives as recognition compounds. In fact, the difference of the ion-selectivity was observed in the fluorescence response of the disubstituted malonamides having two pyrene rings.[7]

2.6. Visual analyses

The adaptability of bisquinolinyl malonamides to visible analyses as the fluoroionophore for the Zn^{2+} ion was also investigated. As mentioned above, the F_{Zn}/F_{Cd} values of the fluorescence intensities to the Zn^{2+} ion against the Cd^{2+} ion increased in the order of malonamide **1** << **3** < **2** < **4**. Visual analysis of malonamide **4** (F_{Zn}/F_{Cd} = 5.5) was carried out and, as comparison, malonamide **1** (F_{Zn}/F_{Cd} = 0.7) was also examined.

Fig. S7 shows digital images of the DMSO solutions of malonamides **1** and **4** obtained by black-light visualization (315 – 400 nm) in the absence or presence of 1 equiv. of each of the Zn^{2+}, Ni^{2+} and Co^{2+}, Cd^{2+},Ca^{2+} ions. The addition of the Cd^{2+} ion rather than the Zn^{2+} ion induced a bright fluorescence of the unsubstituted malonamide **1** (Fig. S7a). On the other hand, the induced fluorescence of malonamide **4** by the addition of the Cd^{2+} ions was significantly inhibited (Fig. S7b). The fluorescence of malonamide **4** with the Zn^{2+} ions, however, was slightly inferior to that of malonamide **1** with the Zn^{2+} ions. This was supported by results showing that the quantum yield of malonamide **4** with the Zn^{2+} ion (Φ_F = 0.168) was superior to that of malonamide **1** with the Zn^{2+} ion (Φ_F = 0.188).[36-40]

In all of the malonamides **1** – **4**, the F_{Zn}/F_{Cd} values using the DMF solvent were superior to those using DMSO solvent (Fig. S3). Thus, visual analyses by DMF solvent for malonamide **4** provided the best results over those by DMSO solvent (Fig. 9b). In contrast, visual analyses with DMF solvent for malonamide **1** showed inferior results to those by DMSO solvent (Fig. 9a).

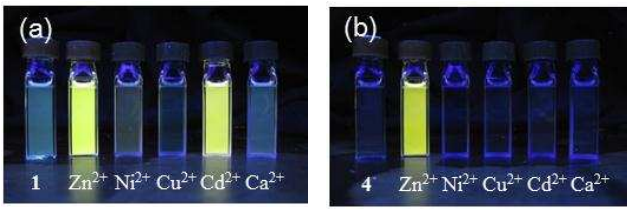

Fig. 9. Digital images of malonamides a) **1** and b) **4** of black-light visualization (315 – 400 nm) of (left to right): malonamide, and malonamide + 1 equiv. of each of the Zn^{2+}, Ni^{2+} and Cu^{2+}, Cd^{2+}, Ca^{2+} ions. [malonamide] = 50 μM in DMF.

In addition, malonamide **4** was applied to fluorescence imaging of the Zn^{2+} ion in vegetable cells. As an essential micronutrient, zinc is need for the normal growth of plants, animals and humans and the zinc-enriched cereal crops can partially compensate zinc deficiency in human body due to the high consumption of cereal crops in developing countries.[41] A layer of epidermal cells of a purple onion was exposed to an

aqueous solution of 50 μM $Zn(CH_3COO)_2$ for 4 h. After sufficient washing with water and wiping dry, the layer was exposed to a DMSO solution of 50 μM malonamide **4** for 4 h. Then, after sufficient washing with DMSO and wiping dry, a fluorescence micrograph of the vegetable cells was taken by an optical microscope. According to the fluorescent properties of malonamide **4**, the optical windows at 360 ± 40 nm (an excitation filter) and 535 ± 50 nm (an emission filter) were utilized for the fluorescence imaging. Fig. 10b is obtained by superimposing the fluorescence image on the bright-field image of Fig. 10a. The Zn^{2+} ions taken from the aqueous solution was shown to be concentrated around the cell nuclei of the purple onion. The fluorescence image obtained could visually reveal the existence of intracellular zinc.

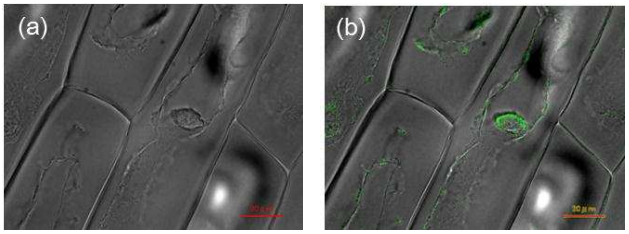

Fig. 10. a) Bright-field image and b) superimposed fluorescence image of vegetable cells were taken after exposure to an aqueous solution of 50 μM $Zn(CH_3COO)_2$ and a DMSO solution of 50 μM malonamide **4**, respectively.

3. Conclusion

In this study, malonamides **1** – **4** possessing two quinoline moieties were designed. The semi-empirical molecular orbital calculations demonstrated that the substituents introduced into the C2-position of malonamides affect the dihedral angles between two quinoline rings. Malonamide **1** without the substituent, which has the widest dihedral angle, displayed Co^{2+} ion selectivity in DMSO solvent. Among malonamides **1** – **4**, only malonamide **4** displayed the highest binding constant and the highest fluorescence intensity in the presence of Zn^{2+} ions as compared with the Cd^{2+} and Co^{2+} ions. However, malonamide **2**, which has a moderate dihedral angle, exhibited the most favorable ratiometric performance for the Zn^{2+} ion since the addition of the Zn^{2+} ion quenched most of the fluorescence of malonamide **2** itself. Although the substituents introduced into the C2-position are spatially distant from the recognition moiety quinoline, this study indicated that they greatly influenced the ion selectivities of bisquinolinyl malonamides.

4. Experimental section

4.1. Reagents and instruments

All reagents were commercially available in the highest grade and used for the syntheses of malonamides as such unless otherwise specified. Ethyl alcohol and pyridine were dried over molecular sieve 4 Å. Benzene and toluene was dried over sodium and distilled. All reactions were carried out under dry nitrogen. Dimethyl sulfoxide (DMSO) and N,N'-dimethyl formamide (DMF) was supplied from Wako Pure Chemical Industries Ltd in the spectrochemical analysis grade for the absorption and fluorescence spectrometries. Metal cations were added to a solution of a malonamide derivative as acetate salts for the absorption and fluorescence spectrometries.

The ^1H and ^{13}C NMR spectra were recorded at 300 and 75 MHz, respectively. Samples for NMR spectra were examined in $CDCl_3$ solutions at 25.0 °C on a Varian 300MHz NMR spectrometer (XL-300). Chemical shifts are given in δ (ppm) relative to deuterated solvents (^{13}C NMR) or to TMS (^1H NMR) as an internal standard. IR spectra were run in KBr discs on a Shimazu FTIR-8600 spectrometer. High-resolution mass (HRMS) spectra (positive mode of EI mass for **1** – **3**, positive mode of FAB mass for **4**) were recorded on a JEOL JMS-DX-303. Fluorescence emission spectra were recorded on a Shimazu RF-5300PC(S) Luminescence Spectrometer. UV-Vis spectra were recorded on a Shimazu MPS-2000 Spectrophotometer. Fluorescence micrographs were recorded on a Keyence BZ-9000 Fluorescence Digital Microscope.

4.2. Preparation of malonamides

*4.2.1. General procedure for the synthesis of malonamides **1** – **4*** A series of bisquinolinyl malonamide derivatives was obtained by the reaction of 8-aminoqinoline with various malonic acid dichlorides. Disubstituted malonic acid dichloride was synthesized by the reaction of the corresponding disubstituted malonic acid with $(COCl)_2$ in benzene or toluene.[6,7]

*4.2.2. N,N'-Bis(8-quinolyl)malonamide (**1**)* 8-aminoquinoline (2.12 g) was dissolved in dry toluene (200 mL). Triethylamine (2.1 mL) and *N,N'*-dimethyl-4-aminopyridine (DMAP) (2.19 g) was added to the solution. In a dark room, the dry toluene solution (40 mL) of unsubstituted malonyl dichloride (1.23 g) was added dropwise to the solution and stirred for 48h at room temperature. Deionized water (50 mL) and chloroform (80 mL) were added to the solution. The solution was extracted with chloroform (100 × 3 mL) and washed with water (50 × 2 mL). The organic layer was dried over anhydrous magnesium sulfate, filtrated and evaporated under reduced pressure. The purification was performed by washing with acetone. Yield: 0.20 g, 6%; white solid; mp 216.0-220.0 °C. IR(KBr): 1678.0 cm^{-1}. ^1H NMR (300MHz NMR, $CDCl_3$): 3.89 (s, 2H), 7.50 (dd, 2H, *J* = 4.40 and 8.25 Hz), 7.54 (dd, 2H, *J* = 3.60 and 7.80 Hz), 7.55 (dd, 2H, *J* = 5.40 and 7.80 Hz), 8.16 (dd, 2H, *J* = 1.65 and 8.25 Hz), 8.86 (dd, 2H, *J* = 3.60 and 5.40 Hz), 8.90 (dd, 2H, *J* = 1.65 and 4.40 Hz), 10.82 (br, 2H). ^{13}C NMR (75MHz NMR, $CDCl_3$): 46.7, 117.1, 121.7, 122.1, 127.2, 127.9, 134.2, 136.2, 138.6, 148.6, 165.1. HRMS (EI+): m/z calcd for $C_{21}H_{16}N_4O_2$ 356.1309, found 356.1275.

*4.2.3. N,N'-Bis(8--quinolyl)-2,2-dimethylmalonamide (**2**)* 8-aminoquinoline (2.2 g) and dry pyridine (2.5 mL) were dissolved in dry benzene (200 mL). In a dark room, the dry benzene solution (40 mL) of 2,2-dimethyl malonyl chloride (1.0 g) was added dropwise to the solution and stirred for 18h at room temperature. Deionized water (50 mL) and chloroform (80 mL) were added to the solution. The solution was extracted with chloroform (100 × 3 mL) and washed with water (50 × 2 mL). The organic layer was dried over anhydrous magnesium sulfate, filtrated and evaporated under reduced pressure. Yield: 0.39 g, 17%; white solid; mp 156.5-163.2 °C. IR(KBr): 1668.3 cm^{-1}. ^1H NMR (300MHz NMR, $CDCl_3$): 1.92 (s, 6H), 7.44 (dd, 2H, *J* = 4.20 and 8.40 Hz), 7.51 (dd, 2H, *J* = 2.10 and 7.50 Hz), 7.52 (dd, 2H, *J* = 6.90 and 7.50 Hz), 8.14 (dd, 2H, *J* = 1.80 and 8.40 Hz), 8.83 (dd, 2H, *J* = 2.10 and 6.90 Hz), 8.86 (dd, 2H, *J* = 1.80 and 4.20 Hz), 10.94 (br, 2H). ^{13}C NMR (75MHz NMR, $CDCl_3$): 24.1, 52.7, 116.7, 121.6, 121.9, 127.2, 127.9, 134.4, 136.1, 138.9, 148.5, 171.6. HRMS (EI+): m/z calcd for $C_{23}H_{20}N_4O_2$ 384.1586, found 384.1582.

*4.2.4. 2-benzyl-2-methyl-malonyl dichloride for **3*** Sodium metal (9.8 g) was added to dry ethyl alcohol (500 mL) at 0°C and stirred for 2.5 h until sodium metal dissolved completely to form sodium ethoxide. Methylmalonic acid diethyl ester (43.7 g) was added dropwise over period of 2 h. The reaction solution was refluxed for 1h. Then benzyl chloride (31.6 g) was added and refluxed for 48 h. After concentration in vacuo for the removal of the solvent, the residue was added by water (50 mL). The solution was extracted with diethyl ether (100×3 mL). The organic layer was dried over anhydrous magnesium sulfate, filtrated and evaporated under reduced pressure. The purification was performed by distillation under reduced pressure to give 2-benzyl-2-methyl-malonic acid diethyl ester. Yield: 3.63 g, 4.2%; pale yellow tough liquid; bp 77.0 °C (0.4 mmHg). ^{1}H NMR (300MHz NMR, $CDCl_3$): 1.20 (t, 6H, *J* = 7.20 Hz), 1.33 (s, 3H), 3.22 (s, 2H), 4.15 (q, 4H, *J* = 7.20 Hz), 7.07–7.33 (m, 5H). ^{13}C NMR (75MHz NMR, $CDCl_3$): 13.54, 19.22, 40.68, 54.34, 60.74, 126.43, 127.70, 129.78, 135.83, 171.30. Sodium hydroxide (10.3 g) was added to dry ethyl alcohol (250 mL) at room temperature and stirred for 1.5 h until sodium hydroxide dissolved completely. The gained 2-benzyl-2-methyl-malonic acid diethyl ester (13.7 g) was added dropwise over period of 1h. The reaction solution was refluxed for 23 h. After the filtration the pale yellow solid was obtained and washed with dry ethyl alcohol. After filtration, the precipitate was dried under reduced pressure. The obtained solid was dissolved in water (150 mL). Then the solution was became pH 1 by the addition of hydrochloric acid to form the precipitate. After filtration, the precipitate was dissolved in diethyl ether (100 mL) and the filtrate was washed with diethyl ether (100 × 3 mL). These diethyl ether solution was washed with water (100 × 2 mL). The organic layer was dried over anhydrous magnesium sulfate, filtrated and evaporated under reduced pressure. The gained solid was washed with hexane to give 2-benzyl-2-methyl-malonic acid. Further purification was performed by recrystallization with acetone. Yield: 8.67 g, 80%; pale yellow crystal. ^{1}H NMR (300MHz NMR, $CDCl_3$): 1.46 (s, 3H), 3.29 (s, 2H), 7.18 (dd, 2H, *J* = 1.80 and 2.40 Hz), 7.27 (d, 3H, *J* = 7.20 Hz). 2-Benzyl-2-methyl-malonic acid (3.49 g) and dry pyridine (2.3 mL) were added in dry benzene (65 mL) and stirred for 2h at room temperature. In a dark room, oxalyl chloride (8.0 mL) was added dropwise and stirred for 22h. Then the reaction solution was refluxed for 24h outside a dark room. After concentration in vacuo for the removal of the solvent, the residue was distilled under reduced pressure to give 2-benzyl-2-methyl malonyl dichloride. Yield: 2.43 g, 59%; pale yellow liquid; bp 76.0 °C (0.1 mmHg). IR (KBr): 1780, 943 cm^{-1}.

*4.2.5. N,N'-Bis(8--quinolyl)-2-benzyl-2-methylmalonamide (**3**)* 8-aminoquinoline (3.3 g) and dry pyridine (5.0 mL) were dissolved in dry benzene (200 mL). In a dark room, the dry benzene solution (40 mL) of 2-benzyl-2-methyl malonyl chloride (2.3 g) was added dropwise to the solution and stirred for 18h at room temperature. Deionized water (50 mL) and chloroform (80 mL) were added to the solution. The solution was extracted with chloroform (100 × 3 mL) and washed with water (50 × 2 mL). The organic layer was dried over anhydrous magnesium sulfate, filtrated and evaporated under reduced pressure. Yield: 1.99 g, 46%; pale yellow solid; mp 150.1-155.7 °C. IR(KBr): 1668.3 cm^{-1}. ^{1}H NMR (300MHz NMR, $CDCl_3$): 1.79 (s, 3H), 3.65 (s, 2H), 7.16-7.30 (m, 5H), 7.44 (dd, 2H, *J* = 4.20 and 8.40 Hz), 7.53 (dd, 2H, *J* = 2.10 and 8.40 Hz), 7.54 (dd, 2H, *J* = 6.75 and 8.40 Hz), 8.14 (dd, 2H, *J* = 1.80 and 8.40 Hz), 8.85 (dd, 2H, *J* = 2.10 and 6.75 Hz), 8.85 (dd, 2H, *J* = 1.80 and 4.20 Hz), 10.94 (br, 2H). ^{13}C NMR (75MHz NMR, $CDCl_3$): 18.5, 44.9, 57.4, 116.8, 121.6, 121.9, 126.9, 127.1, 127.8, 128.2, 130.2, 134.3, 136.1, 136.4, 138.9, 148.5, 170.7. HRMS (EI+): m/z calcd for $C_{29}H_{24}N_4O_2$ 460.1899, found 460.1894.

*4.2.6. N,N'-Bis(8--quinolyl)-2-methyl-2-naphthalenylmethylmalonamide (**4**)* 2-metyl-2-naphthalenylmethymalonyl dichloride was obtained following a published procedure.[7] 8-aminoquinoline (2.9 g) and dry pyridine (5.0 mL) were dissolved in dry benzene (150 mL). In a dark room, the dry benzene solution (30 mL) of 2-benzyl-2-methyl malonyl chloride (3.9 g) was added dropwise to the solution and stirred for 72h at room temperature. 0.5 M hydrochloric acid aqueous solution (30 mL) and chloroform (150 mL) were added to the solution. The solution was extracted with chloroform (50 × 5 mL) and washed with water (50 × 2 mL). The organic layer was dried over anhydrous magnesium sulfate, filtrated and evaporated under reduced pressure. Yield: 1.60 g, 32%; pale yellow crystal; mp 160.1-163.9 °C. IR(KBr): 1691.5 cm^{-1}. ^{1}H NMR (300MHz NMR, $CDCl_3$): 1.83 (s, 3H), 3.81 (s, 2H), 7.33-7.46 (m, 3H), 7.42 (dd, 2H, *J* = 4.20 and 8.40 Hz), 7.52 (dd, 2H, *J* = 1.80 and 8.40 Hz), 7.62-7.78 (m, 4H) , 7.56 (dd, 2H, *J* = 7.20 and 8.40 Hz), 8.13 (dd, 2H, *J* = 1.80 and 8.40 Hz), 8.81 (dd, 2H, *J* = 1.80 and 4.20 Hz), 8.91 (dd, 2H, *J* = 1.80 and 7.20 Hz), 11.11 (br, 2H). ^{13}C NMR (75MHz NMR, $CDCl_3$): 18.5, 45.1, 57.5, 116.8, 121.6, 122.0, 125.5, 125.8, 127.1, 127.4, 127.6, 127.8, 127.8, 128.3, 129.1, 132.4, 133.3, 134.0, 134.3, 136.1, 138.9, 148.6, 170.7. HRMS(FAB+): m/z calcd for $C_{33}H_{26}N_4O_2$ 510.2056, found [M+H] 511.2142.

4.2.7. N-Mono(8-quinolyl)acetamide (***5***) 8-aminoquinoline (2.7 g) was dissolved in dry toluene (200 mL). Triethylamine (4.0 mL) and *N,N'*-dimethyl-4-aminopyridine (DMAP) (0.35 g) was added to the solution. In a dark room, the dry toluene solution (40 mL) of acetyl chloride (2.10 g) was added dropwise to the solution and stirred for 18h at room temperature. After filtration for the removal of the solid, the solution was washed by water (100 × 5 mL). The organic layer was completely evaporated under reduced pressure. Yield: 1.94 g, 57%; pale yellow solid; mp 94.2-96.6 °C. IR(KBr): 1666.4 cm^{-1}. ^{1}H NMR (300MHz NMR, $CDCl_3$): 2.35 (s, 3H), 7.43 (dd, 1H, *J* = 4.20 and 8.40 Hz), 7.47 (dd, 1H, *J* = 1.80 and 8.40 Hz), 7.52 (dd, 1H, *J* = 8.10 and 8.10 Hz), 8.13 (dd, 1H, *J* = 1.50 and 8.40 Hz), 8.77 (dd, 1H, *J* = 1.80 and 8.10 Hz), 8.78 (dd, 2H, *J* = 1.50 and 4.20 Hz), 9.78 (br, 1H). ^{13}C NMR (75MHz NMR, $CDCl_3$): 25.3, 116.4, 121.4, 121.6, 127.4, 127.9, 134.5, 136.4, 138.2, 148.1, 168.8. HRMS (EI+): m/z calcd for $C_{11}H_{10}N_2O$ 186.0793, found 186.0797.

4.3. Fluorescence spectroscopy

Fluorescence emission spectra were recorded at room temperature. A 1 cm × 1 cm quartz cuvette was used for the spectroscopic analysis. Stock solutions of fluoroionophores in DMSO (160 μM) or DMF (200 μM) were prepared for fluorescence detections and diluted to a final concentration of 5.0 μM or 2.0 μM by mixing 500 μM stock solutions of inorganic acetates (CH_3COOLi, CH_3COONa, CH_3COOK, CH_3COONH_4, $Mg(CH_3COO)_2$, $Ca(CH_3COO)_2$, $Al(CH_3COO)_3$, $Mn(CH_3COO)_2$, $Co(CH_3COO)_2$, $Ni(CH_3COO)_2$, $Cu(CH_3COO)_2$, $Zn(CH_3COO)_2$, $Cd(CH_3COO)_2$, and CH_3COOAg). The excitation wavelengths were 345 nm (for DMSO) and 320 nm (for DMF) and the emission spectra from ca. 320 to 700 nm were collected (every 2 nm). Excitation and emission slits width were 5 nm.

Likewise, for the investigation of solvent effects, 100 μM stock solutions of fluoroionophores and inorganic perchlorates in $CH_3CN/CHCl_3$ (9:1, v/v) were prepared. inorganic perchlorates

($LiClO_4$, $NaClO_4$, $KClO_4$, NH_4ClO_4, $Mg(ClO_4)_2$, $Ca(ClO_4)_2$, $Al(ClO_4)_3$, $Mn(ClO_4)_2$, $Co(ClO_4)_2$, $Ni(ClO_4)_2$, $Cu(ClO_4)_2$, $Zn(ClO_4)_2$, $Cd(ClO_4)_2$, and $AgClO_4$. The excitation wavelength was 319 nm (for $CH_3CN/CHCl_3$) and the emission spectra from ca. 320 to 700 nm were collected (every 2 nm). Excitation and emission slits width were 5 nm.

For fluorescence titration measurements, a mass stock solutions of fluoroionophores **1** – **4** and $Zn(CH_3COO)_2$ in DMSO was freshly prepared. 50 μM DMSO solution of fluoroionophores **1** – **4** was added to each measuring flask and a DMSO solution of $Zn(CH_3COO)_2$ was added to each flask that corresponded to 0 – 5 equiv. of zinc. The flasks were then filled up with DMSO to give 5 μM DMSO solution of fluoroionophores **1** – **4** including 0 – 5 equiv. of zinc.

4.4. UV-vis analysis

UV-vis spectra were recorded at room temperature. A 1 cm × 1 cm quartz cuvette was used for the spectroscopic analysis. Stock solutions of malonamide derivatives **1** – **4** in DMSO (2.0 mM) or DMF (200 μM) were prepared for UV-vis spectrophotometric titration and diluted to a final concentration of 0.8 mM by mixing 2.0 mM stock solutions of inorganic acetates. DMSO solutions of $Zn(CH_3COO)_2$ and $Co(CH_3COO)_2$ were added to each solution of malonamide derivatives **1** – **4** that corresponded to 0 – 5 equiv. of zinc and cobalt. A DMSO solutions of $Cd(CH_3COO)_2$ was added to each solution of malonamide derivatives **1** – **4** that corresponded to 0 – 30, 40, 50 or 70 equiv. of cadmium. The concentration dependence of the absorbance, A, at a fixed wavelength fits well to Eq. (1), where A_0 and A_∞ are the absorbance at zero and infinite metal ion concentrations, [M], respectively and $[L]_0$ is an initial concentration of malonamide derivative. The stability constants for complex formations, K, were calculated from the titration data.[32]

$$\mathrm{M} + \mathrm{L} \rightleftharpoons \mathrm{ML}$$

$$A = (A_0 + A_\infty K[\mathrm{M}])/(1 + K[\mathrm{M}]) \qquad (1)$$

$$[\mathrm{M}] = [\mathrm{M}]_0 - [\mathrm{L}]_0 \times (A_0 - A)/(A_0 - A_\infty)$$

The acquired K values from the UV-vis titration data were verified by using the estimated K values from the Job's-plot data (Eq. (2)), where A_{max} is the calculated max absorbance, ε is a molar absorbance coefficient of a complex, and c_{total} is the sum of initial concentrations of metal ions and malonamides respectively.

$$\mathrm{mM} + \mathrm{nL} \rightleftharpoons \mathrm{M_mL_n}$$

$$K = [\mathrm{M_mL_n}]/([\mathrm{M}]^{\mathrm{m}}[\mathrm{L}]^{\mathrm{n}}) \qquad (2)$$

$$[\mathrm{M_mL_n}] = (\mathrm{m} + \mathrm{n})\varepsilon A_{max}/c_{total}$$

Job's-plots for the absorbance were determined by keeping the sum of initial concentrations of metal ions and malonamide derivatives **1** – **4** constant at 0.16 mM and changing the molar ratio of metal ions ($X_M = ([M^{2+}]/([M^{2+}] + [\text{derivative}])$) from 0 to 1. Stock solutions of malonamide derivatives **1** – **4** in DMSO (2.0 mM) were prepared for Job's-plot data and diluted by mixing 2.0 mM stock DMSO solutions of inorganic acetates ($Zn(CH_3COO)_2$, $Cd(CH_3COO)_2$ and $Co(CH_3COO)_2$). Job's-plots indicated that 1:1 complexes are formed.

4.5. Computational studies

The semi-empirical calculations were performed using the program SPARTAN '06 for windows (version 1.1.0) SEMIEMPIRICAL PROGRAM.[33] Geometries and heats of formations were evaluated by the PM3 semi-empirical calculations.[34,35]

Supplementary Material

Supplementary data associated with this article can be found in the online version, at http://dx.doi.org/10.1016/j.tet.2012.11.094. These data include the fluorescence and absorption spectrometries.

References and notes

1. Xu, Z.; Yoon, J.; Spring, D. R. *Chem. Soc. Rev.*, **2010**, *39*, 1996–2006.
2. Lim, N. C.; Freake, H. C.; Brückner, C. *Eur. J.* **2005**, *11*, 38–49.
3. Zolotov, Y. A. *Macrocyclic Compounds in Analytical Chemistry (Chemical Analysis: A Series of Monographs on Analytical Chemistry and Its Applications Vol.143)*; Winefordner, J. D., Ed.; Wiley, New York, 1997; Chp 2, pp. 41-62.
4. Rurack, K. *Spectrochim Acta Part A*, **2001**, *57*, 2161-2195.
5. Frederickson, C. J.; Kasarskis, E. J.; Ringo, D.; Frederickson, R. E. *J. Neurosci. Methods*, **1987**, *20*, 91-103.
6. Moriuchi-Kawakami, T.; Aoki, R.; Morita, K.; Tsujioka, H.; Fujimori, K.; Shibutani, Y.; Shono, T. *Anal. Chim. Acta*, **2003**, *480*, 291-298.
7. Moriuchi-Kawakami, T.; Hisada, Y.; Shibutani, Y. *Chem. Cent. J.*, **2010**, *4*, 7: x1-x6.
8. Hirose, T.; Hiratani, K.; Kasuga, K.; Saito, K.; Koike, T.; Kimura, E.; Nagawa, Y.; Nakanishi, H. *J. Chem. Soc. Dalton Trans.*, **1992**, *18*, 2679- 2683.
9. Rotthaus, O.; LeRoy, S.; Tomas, A.; Barkigia, K. M.; Artaud, I. *Inorg. Chim. Acta*, **2004**, *357*, 2211–2217.
10. Rotthaus, O.; LeRoy, S.; Tomas, A.; Barkigia, K. M.; Artaud, I. *Eur. J. Inorg. Chem.*, **2004**, *7*, 1545-1551.
11. Fang, X. M.; Huo, Y. P.; Wei, Z. G.; Yuan, G. Z.; Huang, B. H.; Zhu, S. Z. *Tetrahedron*, **2013**, *69*, 10052-10059.
12. Suzuki, K.; Sato, K.; Hisamoto, H.; Siswanta, D.; Hayashi, K.; Kasahara, N.; Watanabe, K.; Yamamoto, N.; Sasakura, H. *Anal. Chem.*, **1996**, *68*, 208-215.
13. Dollberg, L. C.; Turro, C. *Inorg. Chem.* **2001,** *40*, 2484-2485.
14. Prabhakar, M.; Zacharias, S. P.; Das, K. S. *Inorg. Chem.* **2005**, *44*, 2585-2587.
15. Zhu, X. A.; Zhang, P. J.; Lin, Y. Y.; and Chen, M. X. *Inorg. Chem.* **2008,** *47*, 7389-7395.
16. Williams, J. N.; Gan, G.; Reibenspies, H. J.; Hancock, D. R. *Inorg. Chem.* **2009,** *48*, 1407-1415.
17. Komatsu, K.; Kikuchi, K.; Kojima, H.; Urano, Y.; Nagano, T. *J. Am. Chem. Soc.*, **2005**, *127*, 10197-10204.
18. Zhou, W.; Li, J.; He, X.; Li, C.; Lv, J.; Li,Y.: Wang, S.; Liu, H.; Zhu, D. *Chem. Eur. J.* **2008**, *14*, 754-763.
19. Lee, Y. D.; Singh, N.; Kim, J. M.; Jang, O, D. *Tetrahedron*, **2010**, *66*, 7965-7969.
20. Zhou, X.; Yu, B.; Guo, Y.; Tang, X.; Zhang, H.; Liu, W. *Inorg. Chem.* **2010,** *49*, 4002-4007.
21. Xue, L.; Liub, C.; Jiang, H. *Chem. Commun*. **2009**, 1061-1063.
22. Zhou, S.; Li, P.; Shi, Z.; Tang, X.; Chen, C.; Liu, W. *Inorg. Chem.* **2012**, *51*, 9226-9231.
23. Yuan, Z. G.; Huo, P. Y.; Nie, L. X.; Fang, M. X.; Zhu, Z. S. *Tetrahedron*, **2012**, *68*, 8018-8023.
24. Wang, Q.; Cahill, M. S.; Blumenstein, M.; Lawrence, S. D. *J. Am. Chem. Soc.* **2006**, *128*, 1808-1809.
25. Legrand, M. Y.; Lee, A.; Barboiu, M. *Inorg. Chem.* **2007**, *46*, 9540-9547.
26. Nishimura, G.; Maehara, H.; Shiraishi, Y.; Hirai, T. *Chem. Eur. J.* **2008**, *14*, 259-271.
27. Ghosh, K.; Adhikari, S.; Chattopadhyay, P. A.; Chowdhury, R. P. *Beilstein J. Org. Chem.* **2008**, *4*, x1-x12.
28. Mikata, Y.; Ugai, A.; Ohnishi, R.; Konno, H. *Inorg. Chem.* **2013**, *52*, 10223-10225.
29. Xiaoyan, Z.; Yu, B.; Guo, Y.; Tang, X.; Zhang, H.; Liu, W. *Inorg.Chem.*, **2010**, *49*, 4002–4007.
30. Chen, H.; Huang, N. *J. Jinan Univ. (Natural Science)*, **1994**, *15*, 86-93.
31. P. Job *Ann. Chim. Applicata*, **1928**, *9*, 113–203.

32. Alfimov, M. V.; Churakov, A. V.; Fedorov, Y. V.; Fedorova, O. A.; Gromov, S. P.; Hester, R. E.; Howard, J. A. K.; Kuz'mina, L. G.; Lednev, I. K.; Moore, J. N. *J. Chem. Soc., Perkin Trans. 2*, **1997**, 2249-2256.
33. Hehre, W. J.; *A Guide to Molecular Mechanics and Quantum Chemical Clculation*, Wavefunction, Irvine, 2003.
34. Stewart, J. J. P. *J. Comput. Chem.*, **1989**, *10*, 209-220.
35. Stewart, J. J. P. *J. Comput. Chem.*, **1989**, *10*, 221-264.
36. The fluorescence quantum yields (Φ_F) were measured relatively to quinine bisulfate in H_2SO_4 solution as standards (Φ_F = 0.546 [33]). The quantum yields of malonamides **1** and **4** were Φ_F = 0.178 for **1** and Φ_F = 0.074 for **4**.
37. Olmsted, J., *J. Phys. Chem.*, **1979**, *83*, 2581-2584.
38. Georgiev, N. I.; Asiri, A. M.; Alamry, K. A.; Obaidb, A. Y.; Bojinov, V. B. *J. Photochem. Photobio. A*, **2014**, *277*, 62– 74.
39. Tang, X.; Peng, X.; Dou, W.; Mao, J.; Zheng, J.; Qin, W.; Liu, W.; Chang, J.; Yao, X. *Org. Lett.*, **2008**, *10*, 3653-3656.
40. LeBel, R. G.; Goring, D. A. I. *J.Chem. Eng. Data*, **1962**, *7*, 100-101.
41. Sinha, S.; Mukherjee, T.; Mathew, J.; Mukhopadhyay, S. K.; Ghosh, S. *J. Photochem. Photobio. A*, **2014**, *277*, 181-186.

Supplementary data

Design of bisquinolinyl malonamides as Zn^{2+} ion-selective fluoroionophores based on the substituent effect

Takayo Moriuchi-Kawakami*, Keita Kawata, Sho Nakamura, Yoshiaki Koyama

and Yasuhiko Shibutani

Department of Applied Chemistry, Faculty of Engineering, Osaka Institute of Technology, 5-16-1 Omiya, Asahi, Osaka 535-8585, Japan. Fax: +81-6-6957-2135; Tel: +81-6-6954-4281.

Corresponding Author

*E-mail: kawakami@chem.oit.ac.jp

Experimental

Fluorescence and absorption spectrometries

All reagents were commercially available in the highest grade for the absorption and fluorescence spectrometries. Dimethyl sulfoxide (DMSO) and N,N'-dimethyl formamide (DMF) was supplied from Wako Pure Chemical Industries Ltd. A malonamide derivative was dissolved in DMSO at 1.6×10^{-4} M or DMF at 2.0×10^{-4} M for the absorption spectrometries. A malonamide derivative was dissolved in DMSO at 5.0×10^{-6} M or DMF at 2.0×10^{-6} M for the fluorescence spectrometries. Metal cations were added to a solution of a malonamide derivative as acetate salts.

Figure S1. Fluorescence spectra of amide **5** (5 μM) in the presence of 1 equiv. of various metal ions in DMSO (excitation wavelength: λ_{ex} = 345 nm).

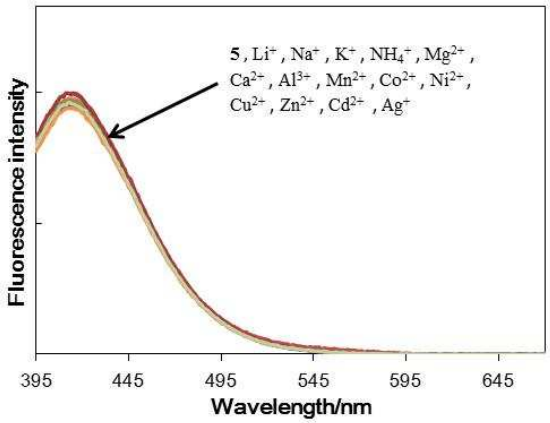

Figure S2. Fluorescence ratiometric response performance of malonamides **2** – **4** (5 μM) in the presence of 1 equiv. of Li^+, Na^+, K^+, NH_4^+, Mg^{2+}, Ca^{2+}, Al^{3+}, Mn^{2+}, Co^{2+}, Ni^{2+}, Cu^{2+}, Zn^{2+}, Cd^{2+}, and Ag^+ in DMSO (excitation wavelength: λ_{ex} = 345 nm): a) **1** (F_{486}/F_{408}), b) **2** (F_{548}/F_{405}), c) **3** (F_{544}/F_{407}), d) **4** (F_{542}/F_{408}).

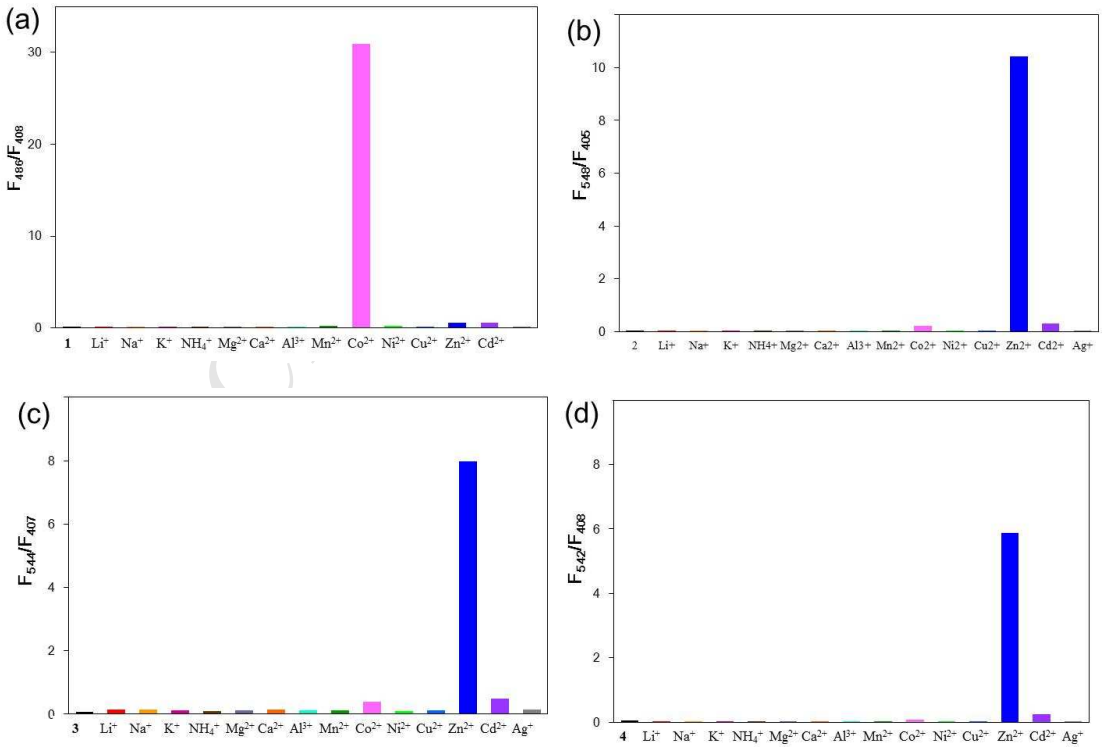

Figure S3. Fluorescence intensity ratios F_{Zn}/F_{Cd} of malonamides **1** – **4** in the presence of the $Zn^{2+}$and Cd^{2+} ions in DMF (gray bar: 2 μM of malonamide with 10 equiv. metal ion, λ_{ex} = 320 nm) and DMSO (black bar: 5 μM of malonamide with 1 equiv. metal ion λ_{ex} = 345 nm).

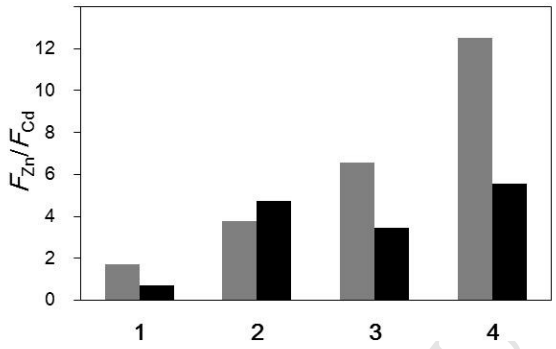

Figure S4. Fluorescence spectra of malonamides **4** in (10 μM) in the presence of 1 equiv. of Li^{+}, NH_4^{+}, Mg^{2+}, Ca^{2+}, Mn^{2+}, Co^{2+}, Ni^{2+}, Cu^{2+}, Zn^{2+}, Cd^{2+}, and Ag^{+} in $CH_3CN/CHCl_3$ (9:1, v/v) (excitation wavelength: λ_{ex} = 319 nm).

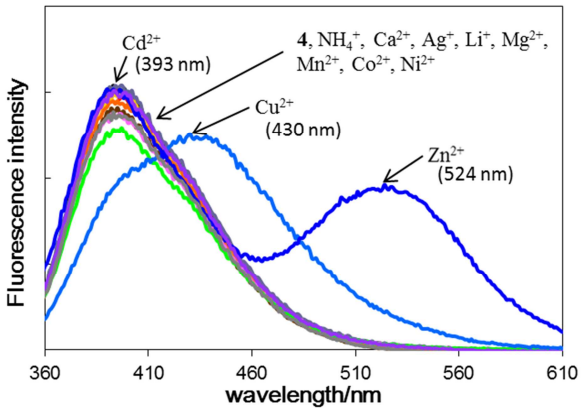

Figure S5. UV-vis absorbance changes of malonamides a) **1**, b) **2**, c) **3**, d) **4** (0.8 mM) obtained during titrations by the Cd^{2+} ion in DMSO.

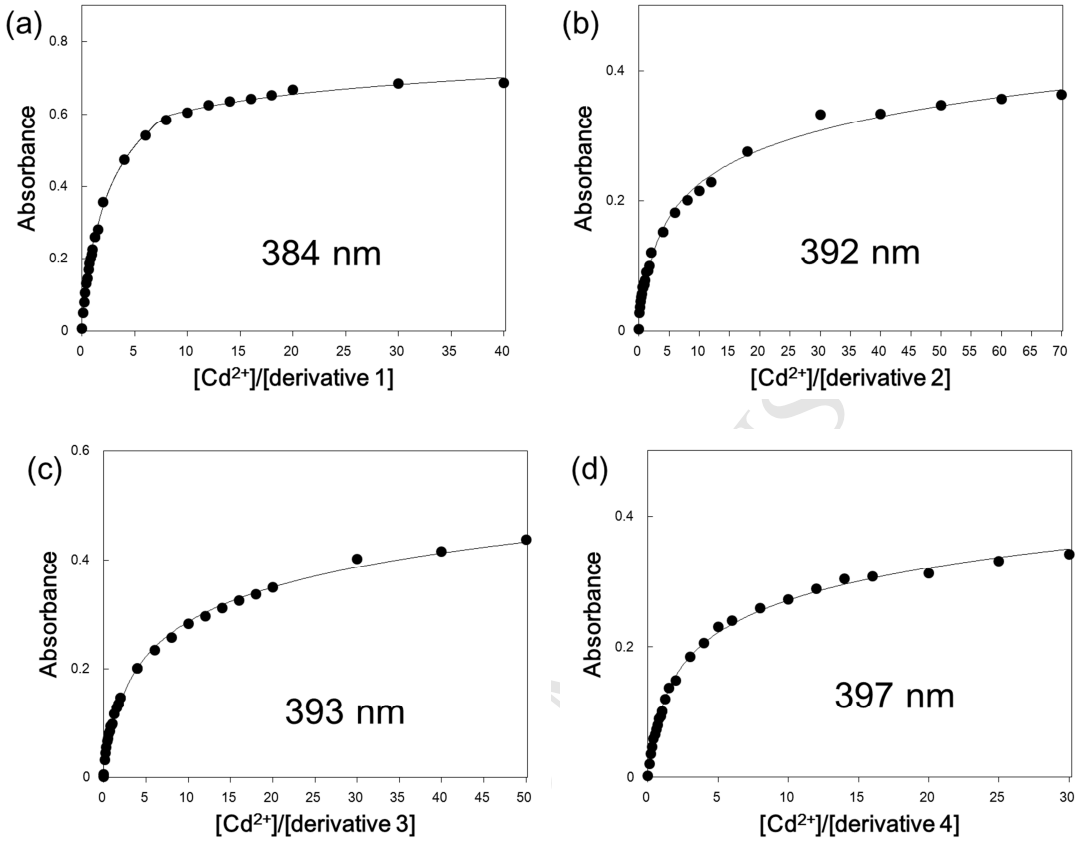

Figure S6. UV-vis absorbance changes of malonamides a) **1**, b) **2**, c) **3**, d) **4** (0.8 mM) obtained during titrations by the Co^{2+} ion in DMSO.

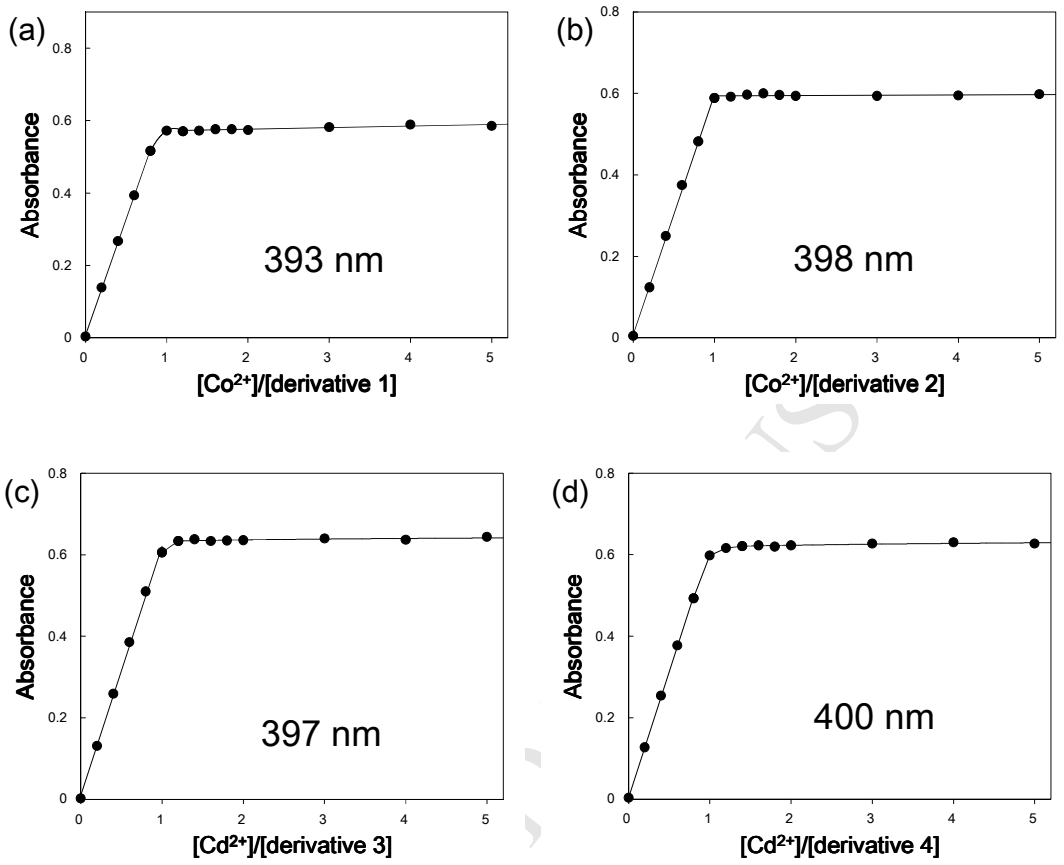

Figure S7. Digital images of malonamides a) **1** and b) **4** of black-light visualization (315 – 400 nm) of (left to right): malonamide, and malonamide + 1 equiv. of each of the Zn^{2+}, Ni^{2+} and Co^{2+}, Cd^{2+},Ca^{2+} ions. [malonamide] = 20 μM in DMSO.